Article

Possibilities of Rock Processing with a High-pressure Abrasive Water Jet with an Aspect Terms to Minimising Energy Consumption

Grzegorz Chomka[1], Maciej Kasperowicz[2], Jarosław Chodór[1*], Jerzy Chudy[2] and Leon Kukiełka[2]

[1] Branch of the Koszalin University of Technology in Szczecinek, Koszalin University of Technology, Waryńskiego 1 Street, 78-400Szczecinek, Poland; grzegorz.chomka@tu.koszalin.pl (G.C.); jaroslaw.chodor@tu.koszalin.pl (J.Cho.)

[2] Faculty of Mechanical Engineering, Koszalin University of Technology, Racławicka 15-17 Street, 75-620 Koszalin, Poland; maciej.kasperowicz@tu.koszalin.pl (M.K); jerzy.chudy@tu.koszalin.pl (J.C.); leon.kukielka@tu.koszalin.pl (L.K.)

* Correspondence: jaroslaw.chodor@tu.koszalin.pl (J.Cho.);

Abstract: Rocks are materials with a wide variety of structures and properties. These can be unprocessed conglomerates of conglomerated minerals as well as crystallized outcrop or metamorphic rocks. Their processing, especially shaping, poses many technological difficulties. Therefore, it is very important to answer the question of how these natural materials yield to high-pressure water jet and abrasive water. It is equally important to determine the effect of key process parameters such as pressure, water nozzle diameter and feed rate on cutting efficiency. The first two parameters determine the water output and power of the jet, while the third determines the jet erosion time per unit volume of material. Their interdependence, using appropriate evaluation indicators, allows to determine the energy intensity of processing and directions for its minimization.

Keywords: high-pressure water jet; high-pressure abrasive water- jet; rock processing

1. Introduction

High-pressure water treatment technology has been developed for more than 50 years. At that time, articles were published on the use of high-pressure water jet to cut through various materials [1 ÷ 6] and high-pressure water jet with additives designed to increase processing efficiency. Ice particles are added to the high-pressure water jet [7 ÷ 10], solidified carbon dioxide particles CO_2 [11, 12], or garnet, corundum or olivine [13 ÷ 16]. High-pressure water jet with dry ice admixtures CO_2 is mostly used for cleaning surfaces [17]. On the other hand, high-pressure waterjet with harder admixtures is used to cut and separate mainly flat titanium materials [18 ÷ 20], heat-resistant steels [21 ÷ 23], austenitic steels [24 ÷ 28], aluminum alloys [29 ÷ 33], copper alloys [34, 35], plastics reinforced with different types of fibers [36 ÷ 39] and glass or ceramics [40 ÷ 42]. There are also reports of research into the use of high-pressure waterjet for cutting through rock materials.

Aydin et al. [43] used granite waste as an abrasive added to the water jet used to cut the marble. It is revealed that the granite particles show similar performance with garnet in terms of the cutting width (granite: 2.10 mm and garnet: 2.21 mm) and the surface roughness (granite: 5.2 μm and garnet: 4.59 μm). It is determined that lower cutting depth (67% of the cutting depth produced by garnet, 15.62 mm) is obtained with the granite particles. Additionally, it is concluded that garnet produces lower kerf angles (70% and 79% of the kerf angle-access and kerf angle-exit produced by the granite particles, respectively). Finally, it can be noted that the granite particles can be effectively used in the cutting of marble and other rocks with similar density and hardness.

Preprints (www.preprints.org) | NOT PEER-REVIEWED | Posted: 9 December 2022 doi:10.20944/preprints202212.0174.v1

Karakurt et al. [44] have identified the main relevant process factors affecting the depth of granite cutting. It was revealed that the sliding speed was the most important process parameters affecting the depth of granite cutting. In addition, it was found that the depth of cut and surface quality were strongly influenced by the grain size and its boundaries with the surrounding grain. In addition, consistent relationships were observed between some of the physical and mechanical properties of granite (for example, water absorption, microhardness, specific bulk density and uniaxial compressive strength) and depth of cut.

Barabas i Florescu [45] presented a method for reducing crack formation during hydro-jet cutting of marble using statistical analysis. A thorough study of the behavior of marble under the hydro-abrasive jet and the behavior of the entire process in processing brittle materials was conducted. Experimental results confirmed the hypothesis that statistical analysis is a procedure that can lead to a reduction in the number of cracks. Reduction in the number of cracks is achieved by using low pressure, a mini-minimum distance from the work surface and a small nozzle diameter.

In paper [46] Huang et al. presented the results of a study of cutting parameters on granite cutting performance. The mass flow rate of the abrasive was found to be proportional only to water pressure, and the effect of other cutting parameters was insignificant. In addition, the increase of water pressure is associated with increased crack width and reduced crack cone. The width of the cut decreases as the nozzle feed rate increases, resulting in a significant increase in the cone of the cut as the nozzle feed rate increases.

The scope of research on the application of high-pressure waterjet is very broad. Some authors [47] present the results of studies of important rock properties affecting the recycling of abrasives in granite cutting. In contrast, others [48 ÷ 52] are conducting research on the disintegration of abrasive materials in water jet processing. Although there has been tremendous recent progress in the development of new machinery, equipment and other technical devices that make water-jet processing more efficient, there is still a lack of comprehensive studies outlining its application to rock cutting. At the same time, no studies capturing simultaneously the results of research on the intensification of rock processing using a pure water jet as well as a water-abrasive jet were also presented. This article therefore responds to existing research gaps.

2. Materials and Methods

There have been many attempts to mathematically represent the efficiency of abrasive cutting, which is commonly referred to as the cutting depth h. One of the first relationships is the equation M. Hashisha [53]:

$$h = \frac{\sqrt{2 \cdot \dot{m}_a \cdot v_a^2}}{8 \cdot R_e \cdot v_p} + \frac{2 \cdot \dot{m}_a \cdot (1-c) \cdot v_a^2}{\pi \cdot v_p \cdot \varepsilon \cdot d_j}, \text{ [mm]}, \quad (1)$$

where:

$\dot{m}_a$ - abrasive flow rate, [g·s^{-1}],
v_a - grain speed, [mm·s^{-1}],
R_e - yield stress, [MPa],
v_p - speed rate, [mm·s^{-1}],
c - a constant that determines the portion of the abrasive mass flow involved in cutting,
ε - specific energy of plastic deformations, [kJ],
d_j - jet diameter, [mm].

It results from a two-way model of the cutting process based on the interpenetration of fatigue cutting at small and large grain impact angles. Unfortunately, this equation does not take into account the size of the abrasive particles or, more importantly, the feed rate. This makes it applicable only to plastic materials with 30 ÷ 40% confidence in the representation of the real state [53].

The empirical relationship created by a group of Japanese scientists [54] more accurately depicts the actual cutting process because it already takes into account most of the

Preprints (www.preprints.org) | NOT PEER-REVIEWED | Posted: 9 December 2022 doi:10.20944/preprints202212.0174.v1

parameters that determine its effectiveness. The initial factors of the equation are the power output, feed rate and distance of the nozzle from the workpiece while the type of workpiece material, type of abrasive and the ratio of abrasive and water output were classified as constant factors conditioning the specifics of the process. The above considerations apply to single-pass cutting, so this parameter is not included in the final form of the equation:

$$h = k_1 \cdot \frac{N_j}{v_p \cdot l} + k_2 \cdot \left(\frac{\dot{m}_a}{\dot{m}_w}\right) \cdot \frac{N_j}{v_p \cdot l}\ , \text{[mm]}, \tag{2}$$

where:

k_1, k_2 - constants determined by the type of rock and abrasive,
N_j - jet power, [kW],
l - distance of the nozzle from the surface of the object, [mm],
$\dot{m}_a$ - abrasive flow rate, [g·s^{-1}],
$\dot{m}_w$ - water flow rate, [g·s^{-1}].

The following equation developed by Rehbindera [55], In turn, it makes the eroding parameters dependent on the pressure p and the diameter of the water nozzle d_w, feed v_p, numbers of passes n and the parameters of the treated granite, i.e., erosion resistance expressed as the ratio of average grain size to compressive strength l/R_c and threshold pressure p_{th}

$$h = f\left\{d_w\left(\frac{p}{p_{th}}, \frac{R_c \cdot p \cdot n}{\mu \cdot l \cdot v_p}\right)\right\}, \text{[mm]}. \tag{3}$$

Another relatively simple relationship [56, 57], applicable to single cuts, takes into account only three basic technological parameters of the cutting process:

$$h = k \cdot \frac{p^a \cdot d_w^b}{v_p^c}\ , \text{[mm]}. \tag{4}$$

However, by appropriately selecting factors a, b, c with values derived from, among other things, the type of material to be processed, the abrasive used, or the abrasive output, they reflect the course of the hydro abrasive cutting process with great confidence [56, 57].

Based on the analysis of the above relationships, it can be concluded that the most significant factor affecting the efficiency of cutting with a high-pressure abrasive jet is its power N_j, represented sometimes in entangled form as the product of the pressure and the diameter of the water nozzle. An important factor is also the feed rate, which determines the actual time the jet affects the surface of the material at a given point. Therefore, these quantities should be given priority in further considerations and experiments carried out.

There are many ways to comparatively represent the energy intensity and energy efficiency of cutting through rock materials with a high-pressure abrasive water jet. This can be used most often E_v specific energy of machining, which is an illustration of the energy expenditure required to remove a unit volume of machined material:

$$E_v = \frac{E_j}{V_e}, \text{[kJ·mm}^3\text{]}, \tag{5}$$

where:

E_j – jet energy, [kJ],
V_e – eroding volume, [mm^3].

In addition to it, you can also meet the specific energy of the intersection Ea expressing the energy required to make a cut with a unit area in the plane of motion of the working tool (water-abrasive jet), expressed by the ratio of power to feed speed and depth of cut:

Preprints (www.preprints.org) | NOT PEER-REVIEWED | Posted: 9 December 2022 doi:10.20944/preprints202212.0174.v1

$$E_a = \frac{N_j}{h \cdot v_p} = \frac{E_j}{h \cdot l} \text{ , [kJ·mm}^{-2}\text{]}, \quad (6)$$

where:

N_j – jet power, [kW],
h – eroding depth, [mm],
v_p – speed rate, [mm·s^{-1}],
E_j – jet energy, [kJ],
l – length of cut, [mm].

The specific energy of cutting is also used E_r describing the amount of energy required to make a cut of unit depth,

$$E_r = \frac{E_j}{h} \text{ , [kJ·mm}^{-1}\text{]}, \quad (7)$$

and ace machining efficiency index, which is the ratio of the power of the jet to the unit depth of the cut obtained:

$$a_s = \frac{N_j}{h} \text{ , [kW·mm}^{-1}\text{]}. \quad (8)$$

At this point, it is important to note the close correlation between the last three indicators. Taking into account that the feed rate is the ratio of the length of the obtained cut to the duration of the cut, the specific energy of the cut can be represented as follows:

$$E_a = \frac{a_s}{v_p} = \frac{E_r}{l} \text{ , [kJ·mm}^{-2}\text{]}. \quad (9)$$

The use of four different comparative energy intensity assessment indicators can create ambiguities and distortions in the evaluation of results. Therefore, they were subjected to the following evaluation:

- specific energy (E_v, kJ·mm^{-3}) is dependent on the volume of the groove, which, with decreasing depth of cut, increases with multiple cuts or a large distance of the nozzle from the workpiece,
- machining efficiency index does not take into account the temporal parameters of the process by which its comparison requires results obtained at a constant feed rate,
- the specific energy of cutting E_r, kJ·mm^{-1} may vary depending on the length of cuts or their duration,
- the specific energy of intersection E_a, kJ·mm^{-2} by capturing energy as a relationship between the power of the jet and the feed rate, eliminates the above disadvantages and fully captures the time-energy aspects of machining.

The objects of the research described in this article are mineral materials and primarily rocks. The division of rocks by geological origin is shown in Table 1. Of the contained minerals, representatives of all rock types were included in the study because of the possibility of comparing the effectiveness of high-pressure abrasive jet treatment of materials that clearly differ in their different structures and properties. These include granite, limestone and marble. In addition, complementary studies to expand insights into rock processing included basalt and sandstone.

Preprints (www.preprints.org) | NOT PEER-REVIEWED | Posted: 9 December 2022 doi:10.20944/preprints202212.0174.v1

Table 1. Division of rocks by geological origin [58].

Group	Magmatic		Sedimentary			Ethamorphic
Type	Deep Rocks	Efflo-rescent	Clastic Sedi-ments	Organic Sedi-ments	Chemical Sedi-ments	(trans-formed)
Kind of Rock	**granite**	porphyry	breccia	**limestone**	travertine	gneiss
	syenite	andesite	sandstone	dolomite	gypsum	serpentinite
	diorite	basalt	clay	chalk	anhydrite	quartzite
	peridotite	tuff	slate	marl	alabaster	**marble**
					bauxite	

Granite - has a full crystalline structure, a texture that is disorderly and massive. It is grayish-white, grayish-yellow or pinkish-red in color. The main components of granite are quartz, orthoclase (potassium feldspar) and dark components (hornblende and augite). It is found in the Sudeten Mountains. Granite is characterized by its high strength. The most durable are fine-grained granites with a large amount of evenly distributed quartz and a small amount of mica. Granite from the Strzegom quarry, illustrated in Figure 1, with the following properties, was used for the study:

Technical specifications of granite:

- specific density - $\varrho = 2.65$ Mg·m^{-3},
- compressive strength - R_c =160÷170 MPa,
- abrasiveness in Deval's drum - M_{DE} = 1.7÷5.5 %
- Mohs hardness - MH = 6÷7.

Figure 1. Granite from the Strzegom quarry.

Limestone - a rock with very diverse origins and properties. Very numerous are organic limestones made up of organic debris of various sizes and inorganic masses of calcium carbonate. When organic remains are recognizable to the naked eye, they are said to be biomorphic structures. Fine-grained limestones with massive textures are called compacted limestones. In addition, there are limestones of chemical origin: oolitic (made up of small, adherent balls of calcite), pelitic (a uniform, compact mass of calcium carbonate).

Technical data of limestone from Morawica quarry shown in Figure 2:

- specific density - $\varrho = 2.75$ Mg·m^{-3},
- compressive strength - R_c = 92÷125 MPa,
- abrasiveness in Deval's drum - M_{DE} = 4.3÷23. 5 %
- Mohs hardness - MH = max. 3.

Preprints (www.preprints.org) | NOT PEER-REVIEWED | Posted: 9 December 2022 doi:10.20944/preprints202212.0174.v1

Figure 2. Limestone from Morawica quarry.

Marble is the name for rocks formed by the re-crystallization of sediments containing calcite or other carbonates, deep in the earth at high temperatures and under considerable pressure. It consists of equal grains of CaCO3, which are closely related and form a homogeneous mass. Marble has a medium-crystalline structure and is extremely resistant to weathering. It is found in the Sudetenland and is colored pink-green, gray, greenish or white. Marbles from the deposit in the area of Stronie Śląskie are called Green and White Marianna and have a spotted-white color while those mined near Slavniovice are white, gray or greenish.

The marble used in the study was Marianna white marble, a view of which is included in Figure 3, with the following parameters:

- specific density - ϱ = ok. 2.72 Mg·m^{-3},
- compressive strength - R_c = 52÷58 MPa,
- abrasiveness in Deval's drum - M_{DE} = 2.7÷7.5 %,
- Mohs hardness - MH = 3.

In addition, samples of sandstone and basalt, i.e. rocks with the highest and lowest strength parameters, were tested for comparative purposes.

Figure 3. Marble from White Marianna quarry.

Analysis of the cutting results of these rocks, which have very different properties due to their different geological origins, will show a complete picture of the effectiveness of high-pressure water-jet processing.

3. Results and Discussion

The research was carried out using an abrasive waterjet cutting system from the US company Ingersoll-Rand of the Hydroabrasives type. This device (Figure 4) is derived from the "Streamline" system. The most essential component of the system is the Ingersoll Rand Streamline high-pressure pump with a capacity of approximately 30 kW and a maximum pressure of 379 MPa. It is a double-acting reciprocating piston pump, hydraulically powered.

Preprints (www.preprints.org) | NOT PEER-REVIEWED | Posted: 9 December 2022 doi:10.20944/preprints202212.0174.v1

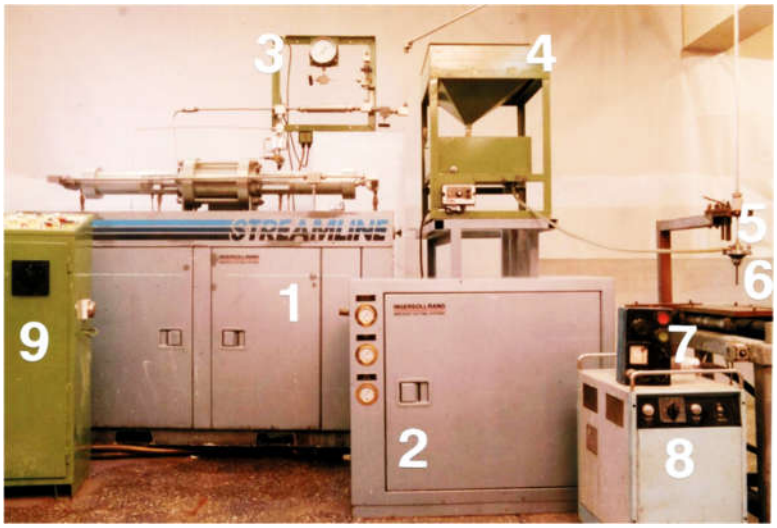

Figure 4. General view of the high-pressure hydroabrasive cutting station: 1-high pressure pump, 2-pre-pump, 3-measuring panel, 4-abrasive feeder, 5-working head, 6-hydroblasting nozzle, 7-working table, 8-table speed controller, 9-control panel.

In the analysis of hydraulic parameters, it is necessary to take into account such basic process factors as water pressure p and the diameter of the water nozzle d_w and the resulting power of the jet N_j. Knowing the influence of these parameters allows to evaluate the energetic aspects of hydro-abrasive cutting of rock materials.

Studies have shown that of the selected rocks, only two succumb to being cut by a stream of clean water. They are sandstone and granite. These rocks are very different from each other. What they have in common is that they are composed of many grains clumped together. The results are shown in Figure 5.

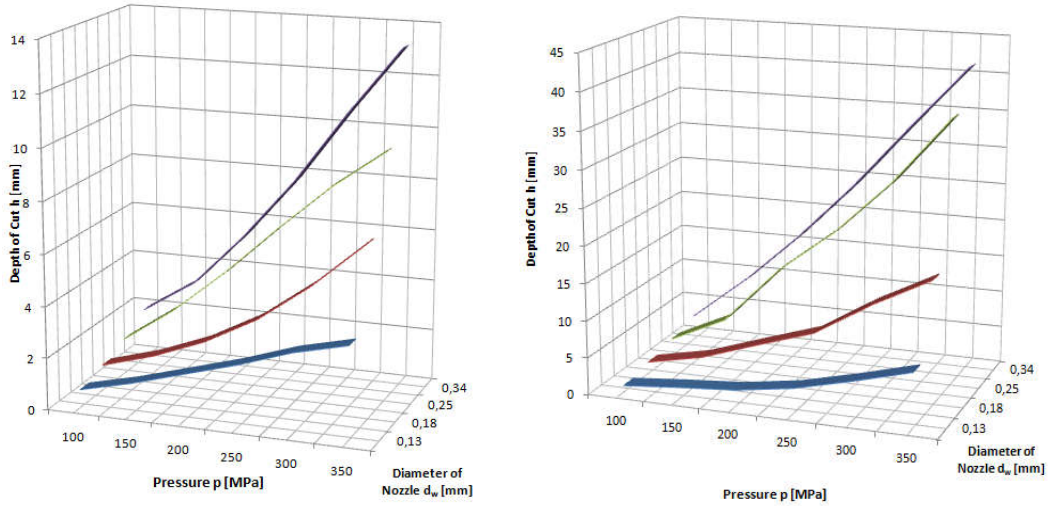

(a) **(b)**

Figure 5. Influence of pressure and water jet diameter on the depth of cut of: **(a)** granite and **(b)** sandstone with a pure water jet: traverse speed v_P = 3 mm·s^{-1}.

The conducted tests showed a linear dependence of the increase in cutting depth on the jet pressure regardless of the type of material being cut. The linear mapping is very accurate as the correlation coefficients are not lower than R=0,985. The graphs in Figure 5 show that as the nozzle diameter increases, the erosion potential of the jet grows stronger. As the pressure increases, the directional coefficients of the straights change from a = 0.011 mm/MPa for nozzle diameter d_w=0.13 mm to a = 0.45 mm/MPa for a d_w=0.34 mm nozzle.

Preprints (www.preprints.org) | NOT PEER-REVIEWED | Posted: 9 December 2022 doi:10.20944/preprints202212.0174.v1

The proportional relationship between pressure and depth of cut is also confirmed by the graphs in Figure 6, which show the results of cutting through rock with an abrasive water jet. In this case, all materials are eroded, and the cutting efficiency is much higher than with a pure water jet.

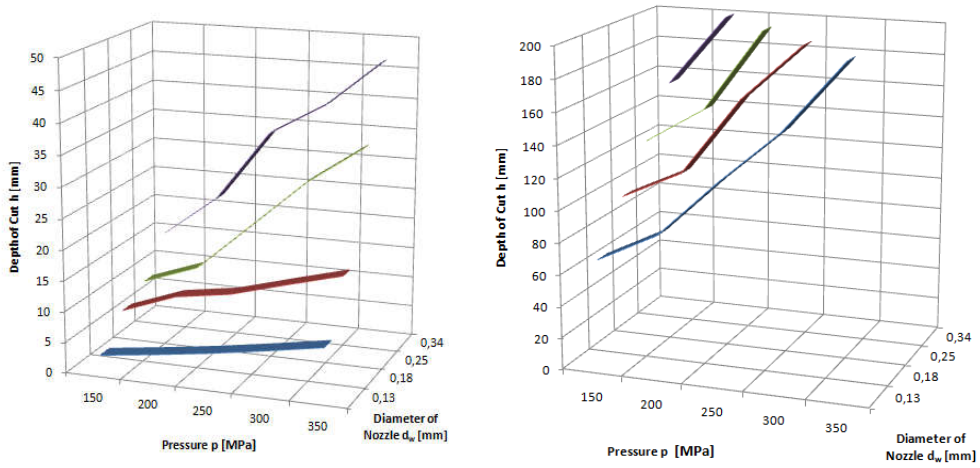

(a) **(b)**

Figure 6. Influence of pressure and water jet diameter on cutting depth of: **(a)** granite; **(b)** sandstone, with abrasive water jet: traverse speed v_P = 3 mm·s^{-1}, abrasive flow rate $\dot{m}_a$ = 6.7 g·s^{-1}.

The highest cutting depths were obtained for sandstone. A 200 mm thick specimen was cut through, for the smallest nozzle with a diameter of d_w=0.13 mm at a maximum pressure of p=350 MPa, for larger ones at much lower pressures. For a nozzle with a diameter of d_w=0.34 mm, the sample was already cut at p=200 MPa.

The most difficult to machine is hard and fine-grained basalt with a compressive strength of $R_c \approx 230$ MPa (Figure 7). Similarly, resistant to such treatment are limestone and marble ($R_c \approx 85 \div 105$ MPa). Slightly better workable is granite, characterized by higher strength parameters than the two previously mentioned rocks ($R_c \approx 110 \div 140$ MPa) and, of course, sandstone with very low parameters $R_c \approx 25 \div 40$ MPa. This is due to the multicomponent structure of these minerals, which determines the specific mechanism of hydro-abrasive erosion. This is a mechanism similar in its course to that occurring in the processing of concrete, and involves the leaching of soft components of these rocks (mica) and the lifting of hard particles (quartz).

Preprints (www.preprints.org) | NOT PEER-REVIEWED | Posted: 9 December 2022 doi:10.20944/preprints202212.0174.v1

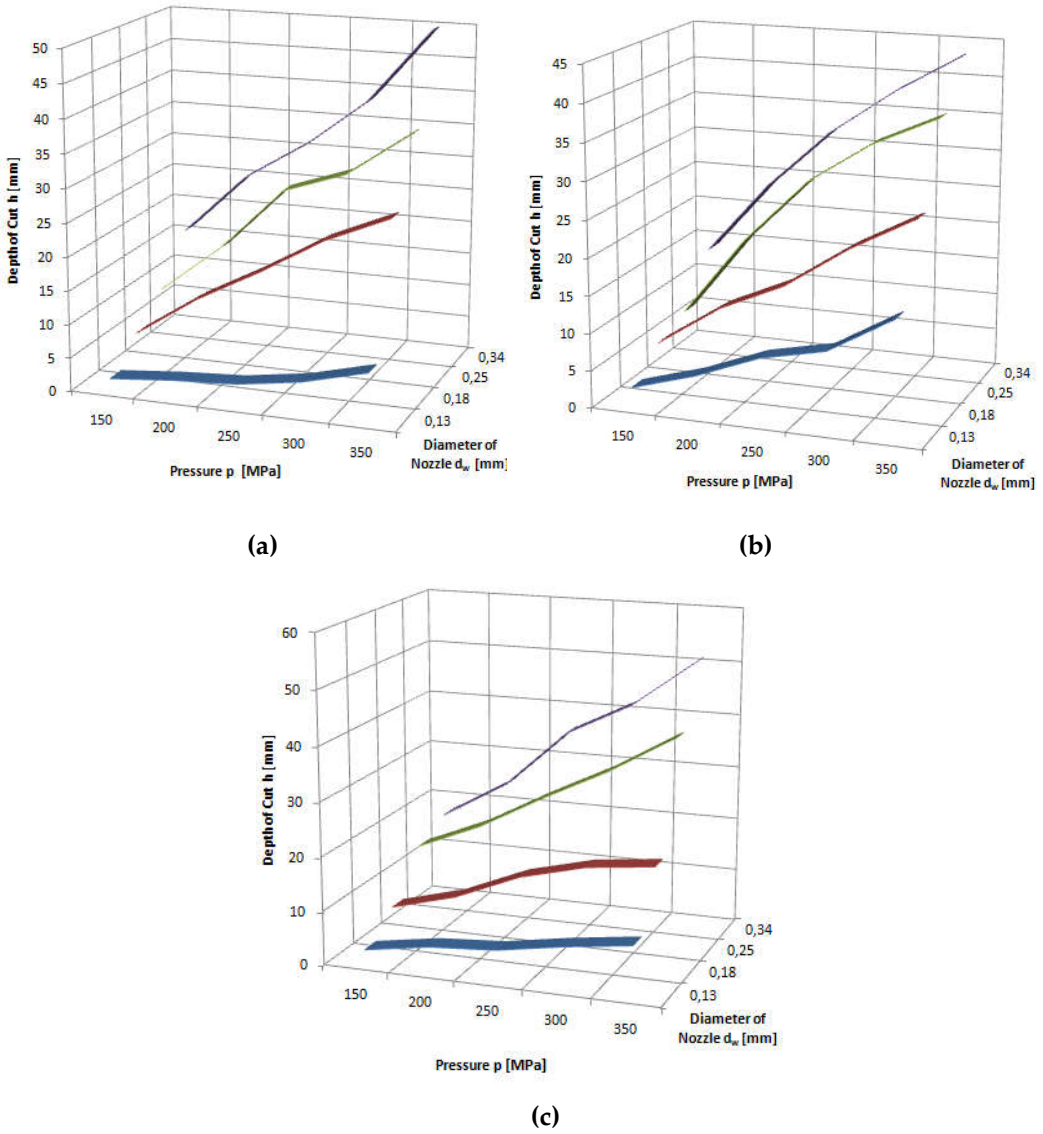

Figure 7. Influence of pressure and water jet diameter on cutting depth of: **(a)** marble; **(b)** basalt;**(c)** limestone, with abrasive water jet: traverse speed $v_P = 3$ mm·s^{-1}, abrasive flow rate $\dot{m}_a = 6.7$ g·s^{-1}.

According to previous considerations and conclusions, the power should most fully reflect the effect of hydraulic parameters on the effectiveness of cutting rock materials because it fully captures aspects of the dynamics of the abrasive hydro jet. The power of the jet can be described as the product of the mass flow rate of the liquid and the square of its velocity according to the following expression:

$$N_j = \frac{\dot{m}_w}{2} \cdot v_w^2 \ , [kW]. \quad (10)$$

It can also be expressed as the product of volumetric water output and its pressure according to the relationship:

$$N_j = V_w \cdot p, [kW]. \quad (11)$$

The nature of these relationships is best illustrated by the dependence of the depth of cut of limestone and granite on the power of the jet shown in Figure 8 and Figure 9. The results of the study are illustrated by nonlinear equations. The accuracy of this mapping

Preprints (www.preprints.org) | NOT PEER-REVIEWED | Posted: 9 December 2022 doi:10.20944/preprints202212.0174.v1

is evidenced by correlation coefficients higher than R = 0,996 each time. Despite the complexity of the results obtained for several types of water nozzle diameters, the observed waveforms are very similar. The directional coefficients of the lines so defined are about a = 2, with a slightly lower one for granite than for limestone. It can be assumed that in the range of pump power up to 30 kW to obtain a cut to a depth of h = 1 mm it takes about 2 kW of pump power.

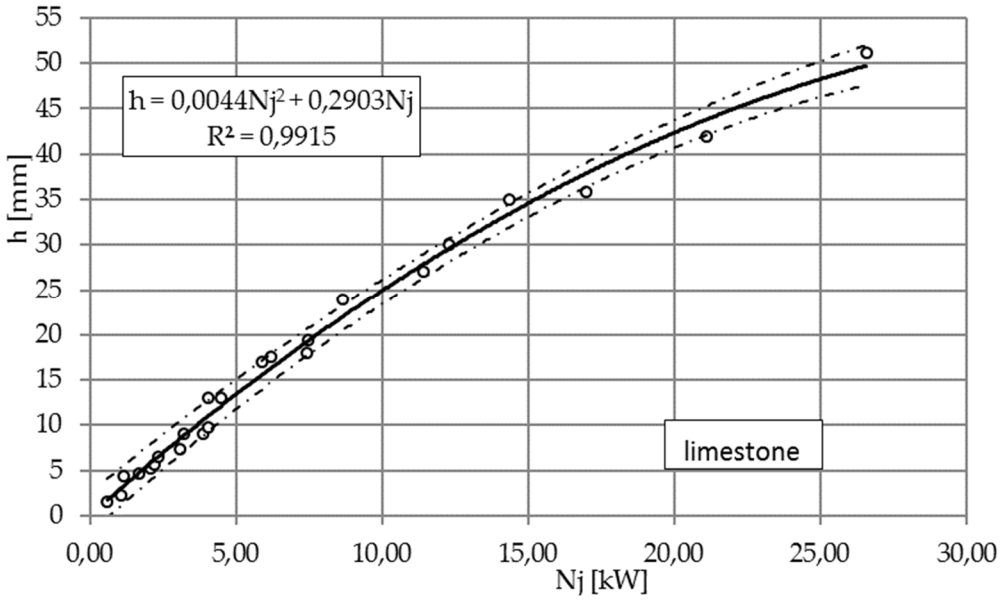

Figure 8. Influence of jet power Nj on cutting depth h of limestone, with abrasive water jet: traverse speed v_P = 3 mm·s^{-1}, abrasive flow rate $\dot{m}_a$ = 6.7 g·s^{-1}.

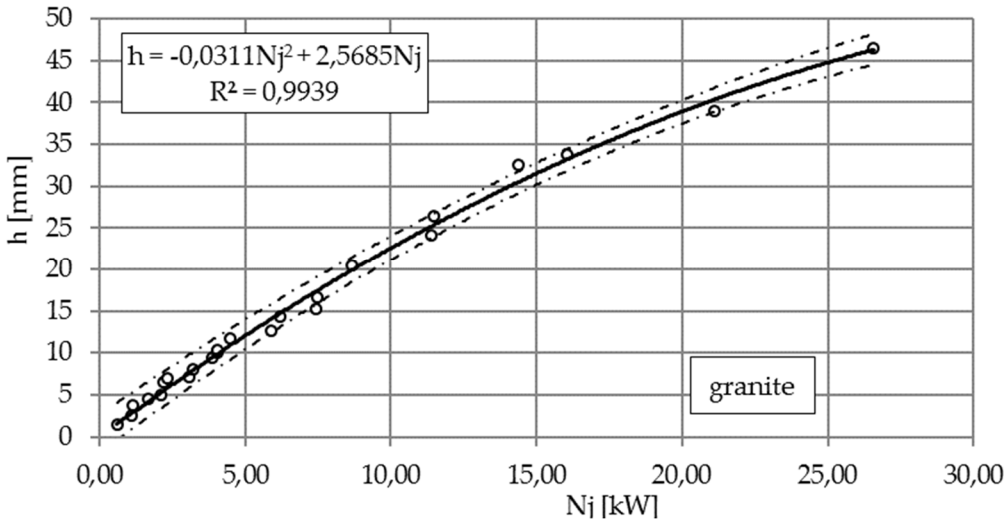

Figure 9. Influence of jet power Nj on cutting depth h of granite, with abrasive water jet: traverse speed v_P = 3 mm·s^{-1}, abrasive flow rate $\dot{m}_a$ = 6.7 g·s^{-1}.

The feed rate is a quantity that determines the penetration time of the high-pressure abrasive jet in a unit volume of material being cut. Thus, an increase in this size induces a decrease in the achievable depth of cut. An illustration of the above can be seen in the charts provided in Figures 10 and Figure 11, for example. These runs have a hyperbolic shape. The power exponents of the functions describing the obtained waveforms are close to minus one, which clearly characterizes the inversely proportional waveforms.

Analyzing these waveforms, it can be concluded that regardless of the pressures used, the highest results are achieved for a feed rate of v_P = 1 mm·s^{-1}. As the jet pressure

Preprints (www.preprints.org) | NOT PEER-REVIEWED | Posted: 9 December 2022 doi:10.20944/preprints202212.0174.v1

increases, the gap depths for this parameter are respectively h = 17.8; 23.5; 44.5; 54.5 and 63.8 mm that is, the spread of extreme values is as high as 46 mm. For feed rate v_p = 12 mm·s^{-1} with the change in pressure, depths of h = 1.9; 2.9; 3.4; 5 reached, respectively, resulting in a more than 10-fold scatter of just 4.1 mm.

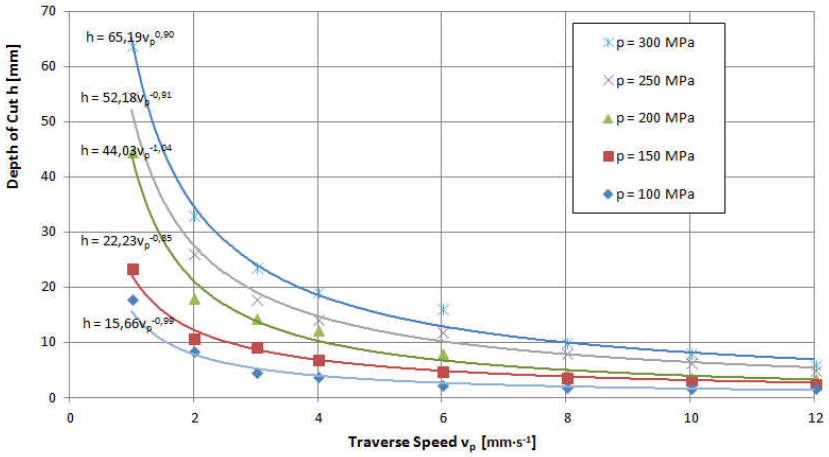

Figure 10. Influence of traverse speed and pressure on the depth of cut of limestone: nozzle diameter d_w=0.25 mm, flow of abrasive $\dot{m}_a$ = 6.7 g·s^{-1}.

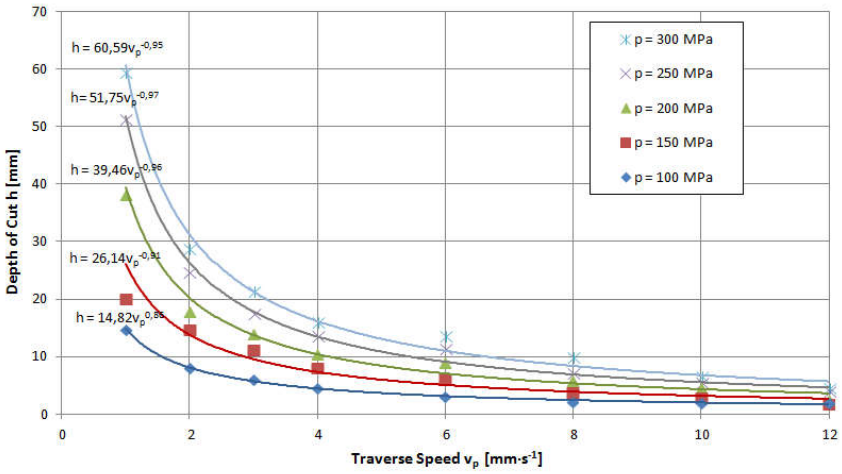

Figure 11. Influence of traverse speed and pressure on the depth of cut of granite: nozzle diameter d_w=0.25 mm, flow of abrasive $\dot{m}_a$ = 6.7 g·s^{-1}.

The energy intensity of the process is determined primarily by the power consumed by the high-pressure pump. It can vary in the apparatus used, depending on the pressure values used and the diameter of the water nozzle, from p = 0.6 to 30 kW. The other equipment, i.e. the pre-pump, abrasive feeder and work table, needs an approximately constant amount of power, amounting to a maximum of p = 1.5 kW. Thus, an assessment aimed at minimizing energy consumption will include only the hydraulic parameters of the structure, treating its other consumption as a constant factor, independent of current processing conditions.

The specific energy of the intersection E_a [59] expressing the energy input required to make an intersection with a unit lateral area of the eroded slot, previously described by equation 6 was used as the main evaluation index.

The choice of this indicator was determined by its adequacy in a situation of varying both hydraulic parameters and machining conditions. This allows the results presented to be unambiguous, which should give maximum clarity to the analysis.

Preprints (www.preprints.org) | NOT PEER-REVIEWED | Posted: 9 December 2022 doi:10.20944/preprints202212.0174.v1

The energy level of the jet is actually determined by two quantities only. These are the pressure of the liquid and the diameter of the water nozzle. By selecting their respective sizes, the speed of the water jet, its output and power are determined.

Experimental tests were carried out in accordance with the five-level rotatable experiment plan experiment plan. Three fold repeatability of the tests was used. This task required following steps to be conducted [17, 60]:

1. Determination of variability range of the studied parameters.
2. Choice of the class of the mathematical model.
3. Coding the analyzed parameters.
4. Gathering the experiment results.
5. Elimination of results with gross mistakes.
6. Calculating the inter-row variance and standard deviation.
7. Checking the homogeneity of variance.
8. Calculating the coefficients of regression function.
9. Statistical analysis of the regression function.
10. Examination of the significance level of the correlation coefficient.
11. Checking the adequacy of the mathematical model.
12. Decoding the regression function.

The average values of the outputs of the object $\overline{E}_a$ were approximated with a a polynomial of the second degree, obtaining the regression equation as two-parameter functions:

$$\hat{\overline{E}}_a = b_o + b_1 \cdot \bar{p} + b_2 \cdot \bar{d}_w + b_{11} \cdot \bar{p}^2 + b_{22} \cdot \bar{d}_w{}^2, \quad [kJ \cdot mm^{-2}] \tag{12}$$

where: $\bar{x}_1{}^2$

b_o, b_1, b_2, b_{11} and b_{22} – unknown coefficients of the regression equation,

$\bar{x}_i$ – input variables: $\bar{x}_1 = \bar{d}_w$ [mm] and $\bar{x}_2 = \bar{p}$ [MPa] or: $\bar{x}_1 = \bar{N}_j$ [kW] and : $\bar{x}_2 = \bar{v}_p$ [mm·s^{-1}].

Using matrix calculus, the column vector {b} of the unknown coefficients in Equation (12) was calculated from the matrix formula:

$$\{b\} = ([\overline{X}]^T[\overline{X}])^{-1}[\overline{X}]^T\{\overline{Y}\}, \tag{13}$$

where:

$[\overline{X}]$ – input variable matrix of dimension N×L. For data N=5 and L=5, the following matrix forms $[\overline{X}]$ were developed,

$[\overline{X}]^T$ – transposed matrix $[\overline{X}]$,

$([\overline{X}]^T[\overline{X}])^{-1}$– covariance matrix,

$\{\overline{Y}\}$ – column vector of the average values of the experimental results.

The boundaries of the confidence region for Regression Function (12) were determined from the following formula:

$$\hat{\overline{E}}_a \pm t_{kr(\alpha;f=N-L)} \cdot \frac{S_R}{\sqrt{N-L-1}} \cdot \sqrt{\{\bar{x}\}^T([\overline{X}]^T[\overline{X}])^{-1}\{\bar{x}\}}, \quad [kJ \cdot mm^{-2}] \tag{14}$$

where:

$\hat{\overline{E}}_a$– regression equation according to Formula (12),

$t_{kr(\alpha;f)}$ – critical value of Student t test for significance level α=0.05 and the number of the degrees of freedom f=N-L,

N – number of measurement points in the experimental design: N=13,

L – number of unknown coefficients in Regression Equation (12); here, L=5,

$\{\bar{x}\}$ and $\{\bar{x}\}^T$– column vector of the functions of input variables (test factors in real form) and its transposition: $\{\bar{x}\}^T = [1\ \bar{x}_1\ \bar{x}_2\ \bar{x}_1{}^2\ \bar{x}_2{}^2]$,

$S_R = \sum_{i=1}^{i=N}(\hat{\bar{y}}_i - \bar{y}_i)^2$– residual variance,

$\hat{\bar{y}}_i$– average values of model outputs for plan points calculated from Equation (12): $(\bar{y}_i = \hat{\overline{E}}_a)$,

$\bar{y}_i$ – average values of experimental results.

The test results after statistical processing according to the algorithm presented in the study [17, 60] were used to develop regression equations (15) and (16).

And these parameters, in turn, determine the course and efficiency of mixing of water and abrasive that is, in the end, the value of energy transferred to individual abrasive

Preprints (www.preprints.org) | NOT PEER-REVIEWED | Posted: 9 December 2022 doi:10.20944/preprints202212.0174.v1

particles determining their micro-cutting abilities. Therefore, Figure 12 just shows the effect of pressure and diameter of the water jet on the level of energy consumption of cutting granite with a high-pressure abrasive hydro jet. The results obtained are illustrated by a surface with the following equation:

$$E_a = -1.08^{-7}p^2 + 2.834d_w^2 + 7.438^{-5}p - 1.436d_w + 0.248 \quad [kJ{\cdot}mm^{-2}] \qquad (15)$$

where: $150 \le p \le 350$ MPa; $0.1 \le d_w \le 0.3$ mm.

In the considered range of parameters, it has a clear minimum, running aong the value of the diameter of the water nozzle calculated from the partial derivative according to the d_w variable and equal to d_w=0.2537 mm. This optimum is quite pronounced. Decreasing or increasing the diameter of the water nozzle entails a similar pronounced increase in the Ea index according to the course of a power function with a quadratic exponent. A much smoother increase in energy intensity entails intensifying processing by increasing pressure. or the maximum difference in applied pressures, the increase is only about 0.02 kJ·mm^{-2}. This is also evidenced by the coefficient at the pressure square factor of only.

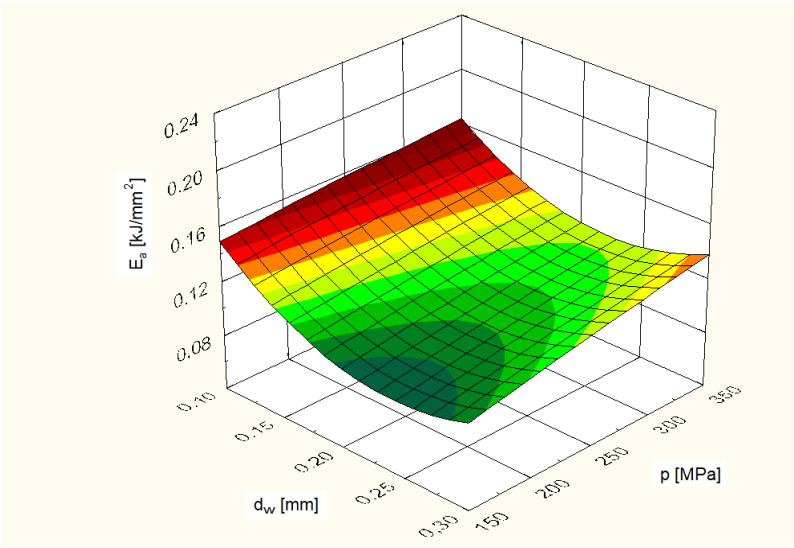

Figure 12. Influence of pressure and water jet diameter on the energy consumption of granite with abrasive water jet: traverse speed v_p = 3 mm·s^{-1}, flow of abrasive $\dot{m}_a$ = 6.7 g·s^{-1}.

The last issue related to optimization according to the criterion of minimizing energy intensity is the answer to the question of whether it is more beneficial to intensify the process with an increase in the power of the water jet or an increase in erosion time. A graphic illustration of this response can be seen in the example surface shown in Figure 13.

Preprints (www.preprints.org) | NOT PEER-REVIEWED | Posted: 9 December 2022 doi:10.20944/preprints202212.0174.v1

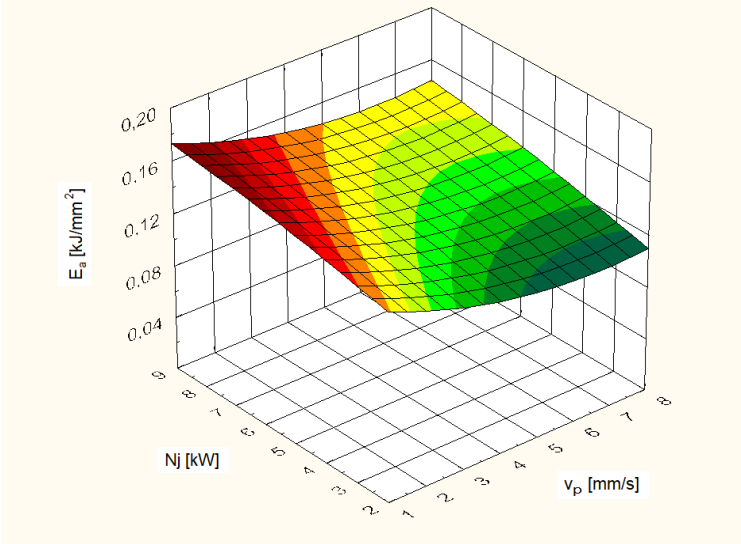

Figure 13. Influence of jet power and traverse speed on the energy consumption of granite with abrasive water jet: traverse speed v_P = 3 mm·s^{-1}, flow of abrasive $\dot{m}_a$ = 6.7 g·s^{-1}.

The described tests were carried out for an optimal water nozzle diameter of d_w=0.25 mm. The resulting surface (with the equation shown below):

$$E_a = -0.001v_p^2 + 0.006N_j - 0.015v_p + 0.146\,, \qquad [kJ{\cdot}mm^{-2}] \tag{16}$$

where: $1 \le v_P \le 8$; mm·s^{-1} and $1 \le N_j \le 9$, kW,

reaches the lowest values for the lowest power and feed rate in the limit of v_p=7.5 mm·s^{-1}. Intensification by both increasing power and decreasing feed rate increases relative power consumption by a similar amount.

4. Conclusions

In summary, it can be concluded that the least energy-intensive method of cutting is the use, for the highest possible pressure, of an optimal water nozzle diameter of d_w=0.25 mm for the tested pump of about 30 kW. Unfortunately, in this way the maximum capacity of the pump can be reached very quickly, which limits the possibilities of intensification. This entails achieving deeper cuts by increasing erosion time through decreasing the feed rate or using multiple passes. The first option is more favorable because it brings a slight increase in the energy intensity of the cutting process at 35% to a value of E_a=0.17 kJ·mm^{-2}. The use of multiple passages has worse results, the increase in energy intensity is rapid and reaches maximum values of E_a=0,35 kJ·mm^{-2}.

Author Contributions: The individual contributions of the Authors: conceptualization, J.Cho., G.C., M.K. and J.C.; methodology, L.K., G.C., J.C and M.K.; investigation, J.Cho., G.C., J.C. and M.K.; software, J.Cho., G.C., J.C., L.K. and M.K.; data curation, G.C., J.C.; validation, J.Cho. and L.K.; writing—original draft preparation, J.Cho., G.C., J.C., L.K. and M.K.; writing—review and editing, J.Cho., G.C., J.C and L.K.; visualization, G.C., J.C.and M.K.; supervision, L.K.; All the Authors have read and agreed to the published version of the manuscript.

Institutional Review Board Statement: Not applicable.

Informed Consent Statement: Not applicable.

Data Availability Statement: Data sharing is not applicable to this article.

Conflicts of Interest: The authors declare no conflict of interest.

 doi:10.20944/preprints202212.0174.v1

References

1. Oertel, J.; Gaab, M.R.; Warzok, R. et al. Waterjet dissection in the brain: review of the experimental and clinical data with special reference to meningioma surgery. *Neurosurg Rev* 26, **2003**, 168–174. . [Google Scholar] [CrossRef]
2. Hreha, P.; Hloch, S.; Magurova, D.; Valicek, J.; Kozak, D.; Harnicarova, M.; Rakin, M. Water jet technology used in medicine. in *Tehnicki vjesnik*. **2010**; 17 (2), 237-240. [Google Scholar] [CrossRef]
3. Alitavoli, M.; McGeough, J.A. An expert process planning system for meat cutting by high pressure water-jet, *Journal of Materials Processing Technology*, **1998**, Volume 84, Issues 1–3, 130-135. [Google Scholar] [CrossRef]
4. Sitek, L.; Bodnárová, L.; Válek, J.; Zeleňák, M.; Klich, J.; Foldyna, J.; Novotný, M. Effects of Water Jet on Heat-Affected Concretes, *Procedia Engineering*, **2013**, Volume 57, 1036-1044. [Google Scholar] [CrossRef]
5. Kasperowicz, M.; Chomka, G.; Chudy, J. Determining the supply pressure depending on the feed speed and the diameter of the nozzle. *Carpathian Journal of Food Science and Technology*, **2018**, Vol. 10/5, pp. 17-23. [Google Scholar]]
6. Kasperowicz, M.; Chomka, G.; Bil, T. Determination of supply pressure during cutting fish using high-pressure water stream taking into account the place and diameter of the water nozzle. DEGRUYTER Cutting, *International Journal of Food Engineering*, **2019**, 16(3). [Google Scholar] [CrossRef]
7. McGeough, JA. Cutting of food products by iceparticles in a water-jet, *Procedia CIRP*, **2016**, 42, 863-865. [Google Scholar] [CrossRef]
8. Deo, A., Bagal, D. K., Pattanaik, A. K., Panda, S. N., Barua, A., Barkey, R. K., & Jeet, S. Recent advancements in ice jet machining process as an alternative of AWJM. *Materials Today: Proceedings*, **2022**, 50, 981-985. [Google Scholar] [CrossRef]
9. Gupta, K., Avvari, M., Mashamba, A., & Mallaiah, M. Ice jet machining: a sustainable variant of abrasive water jet machining. In Sustainable Machining, Springer, Cham., **2017**, 67-78. [Google Scholar] [CrossRef]
10. Huang, F., Mi, J., Li, D., Wang, R., & Zhao, Z. Comparative investigation of the damage of coal subjected to pure water jets, ice abrasive water jets and conventional abrasive water jets. *Powder Technology*, **2021**, 394, 909-925. [Google Scholar] [CrossRef]
11. Spur, G.; Uhlmann, E.; Elbing, F. Dry-ice blasting for cleaning: process, optimization and application. *Wear*, **1999**, Vol. 233-235, 402-411. [Google Scholar] [CrossRef]
12. Chomka, G.;Chudy, J. Analysis and interpretation of measurements of surface machining effectiveness in the process of varnish removal by a water-ice jet. *TehnickiVjesnik-Technical Gazette*. **2013**, 20/5, 847-852, ISSN 1330-3651 (Print), ISSN 1848-6339 (Online). [Google Scholar] [CrossRef]
13. Valíček, J.; Harničárová, M.; Hlavatý, I.; Grznárik, R.; Kušnerová, M.; Hutyrová, Z.; Panda, A. A new approach for the determination of technological parameters for hydroabrasive cutting of materials. *Mater. Werkst*. **2016**, 47, 462–471. [Google Scholar] [CrossRef]
14. Nag, A.; Ščučka, J.; Hlaváček, P.; Klichová, D.; Srivastava, A.K.; Hloch, S.; Dixit, A.R.; Foldyna, J.; Zelenak, M. Hybrid aluminium matrix composite AWJ turning using olivine and Barton garnet. *Int. J. Adv. Manuf. Technol*. **2017**, 94, 2293–2300. [Google Scholar] [CrossRef]
15. Martín, C.G.; Lauand, C.; Hennies, W.; Ciccu, R. Abrasives in Water Jet Cutting Systems; Informa UK Limited: London, UK, **2018**; 641–645. [Google Scholar]
16. Perec, A.; Pude, F.; Grigoryev, A.; Kaufeld, M.; Wegener, K. A study of wear on focusing tubes exposed to corundum-based abrasives in the waterjet cutting process. *Int. J. Adv. Manuf. Technol*. **2019**, 104, 2415–2427. [Google Scholar] [CrossRef]
17. Chomka, G.; Chodór, J.; Kukiełka, L.; Kasperowicz, M. The Use of a High-Pressure Water-Ice Jet for Removing Worn Paint Coating in Renovation Process. *Materials* **2022**, 15, 1168. [Google Scholar] [CrossRef]
18. Perec, A. Experimental research into alternative abrasive material for the abrasive water-jet cutting of titanium. *Int J Adv Manuf Technol* 97, **2018**, 1529–1540. [Google Scholar] [CrossRef]
19. Boud, F.; Carpenter, C.; Folkes, J.; Shipway, P.H. Abrasive waterjet cutting of a titanium alloy: The influence of abrasive morphology and mechanical properties on workpiece grit embedment and cut quality, *Journal of Materials Processing Technology*, **2010**, Vol. 210, Issue 15, 2197-2205. [Google Scholar] [CrossRef]
20. Kong, MC.; Axinte, D. Response of titanium aluminide alloy to abrasive waterjet cutting: Geometrical accuracy and surface integrity issues versus process parameters. *Proceedings of the Institution of Mechanical Engineers, Part B: Journal of Engineering Manufacture*. **2009**, 223 (1):19-42. [Google Scholar] [CrossRef]
21. Patel, D.; Tandon, P. Experimental investigations of thermally enhanced abrasive water jet machining of hard-to-machine metals, *CIRP Journal of Manufacturing Science and Technology*, **2015**, Vol. 10, 92-101. [Google Scholar] [CrossRef]
22. Meshcheryakov, A.V.; Shulepov, A.P. Productivity of abrasive water-jet machining. *Russ. Engin. Res. 37*, **2017**, 747–750. [Google Scholar] [CrossRef]
23. Perec, A.; Pude, F.; Grigoryev, A. et al. A study of wear on focusing tubes exposed to corundum-based abrasives in the waterjet cutting process. *Int J Adv Manuf Technol 104*, **2019**, 2415–2427. [Google Scholar] [CrossRef]
24. Supriya, S.B.; Srinivas, S. Machinability Studies on Stainless steel by abrasive water jet -Review, *Materials Today: Proceedings*, **2018**, Vol. 5, Issue 1, Part 3, 2018, 2871-2876. [Google Scholar] [CrossRef]
25. Löschner, P.; Jarosz, K.; Niesłony, P. Investigation of the effect of cutting speed on surface quality in abrasive water jet cutting of 316L stainless steel. *Procedia Engineering*, **2016**, 149, 276-282. [Google Scholar] [CrossRef]
26. Akkurt, A.; Kulekci, M. K.; Seker, U.; Ercan, F. Effect of feed rate on surface roughness in abrasive waterjet cutting applications. *Journal of Materials Processing Technology*, **2004**, 147. 3, 389-396. [Google Scholar] [CrossRef]

27. Kmec, J.; Gombár, M.; Harničárová, M.; Valíček, J.; Kušnerová, M.; Kříž, J.; Kadnár, M.; Karková, M.; Vagaská, A. The Predictive Model of Surface Texture Generated by Abrasive Water Jet for Austenitic Steels. *Appl. Sci*. **2020**, 10, 3159. [Google Scholar] [CrossRef]
28. Llanto, J. M.; Tolouei-Rad, M.; Vafadar, A.; Aamir, M. Impacts of Traverse Speed and Material Thickness on Abrasive Waterjet Contour Cutting of Austenitic Stainless Steel AISI 304L. *Appl. Sci*. **2021**, 11, 4925. [Google Scholar] [CrossRef]
29. Ahmed, T.M.; Mesalamy, AS El.; Youssef, A.; Midany, T.T. El, Improving surface roughness of abrasive waterjet cutting process by using statistical modeling, *CIRP Journal of Manufacturing Science and Technology*, **2018**, Vol. 22, 30-36. [Google Scholar] [CrossRef]
30. Jegaraj, J.J.R.; Babu, N.R. A soft computing approach for controlling the quality of cut with abrasive waterjet cutting system experiencing orifice and focusing tube wear, *Journal of Materials Processing Technology*, **2007**, Vol. 185, Issues 1–3, 217-227. [Google Scholar] [CrossRef]
31. Yuvaraj, N.; Kumar, M. P. Cutting of aluminium alloy with abrasive water jet and cryogenic assisted abrasive water jet: A comparative study of the surface integrity approach. *Wear*, **2016**, 362, 18-32. [Google Scholar] [CrossRef]
32. Wang, S.; Hu, D.; Yang, F.; Lin, P. Research on Kerf error of aluminum alloy 6061-T6 cut by abrasive water jet. *The International Journal of Advanced Manufacturing Technology*, **2022**, 118(7), 2513-2521. [Google Scholar] [CrossRef]
33. Wang, S.; Hu, D.; Yang, F.; Lin, P. Investigation on kerf taper in abrasive waterjet machining of aluminium alloy 6061-T6. *Journal of Materials Research and Technology*, **2021**, 15, 427-433. [Google Scholar] [CrossRef]
34. Hlaváček, P.; Valíček, J.; Hloch, S.; Greger, M.; Foldyna, J.; Ivandić, Ž.; Zeleňák, M. Measurement of fine grain copper surface texture created by abrasive water jet cutting. *Strojarstvo: časopis za teoriju i praksu u strojarstvu*, **2009**, 51(4), 273-279. [Google Scholar]
35. Spadło, S.; Krajcarz, D. Study of the geometrical structure of copper surface after abrasive waterjet cutting. In *IOP Conference Series: Materials Science and Engineering*, **2018**, Vol. 461, No. 1, p. 012045. [Google Scholar] [CrossRef]
36. Wang, J.; Guo, D. M. A predictive depth of penetration model for abrasive waterjet cutting of polymer matrix composites. *Journal of materials processing technology*, **2002**, 121(2-3), 390-394. [Google Scholar] [CrossRef]
37. Ramulu, M.; Arola, D. The influence of abrasive waterjet cutting conditions on the surface quality of graphite/epoxy laminates. *International Journal of Machine Tools and Manufacture*, **1994**, 34(3), 295-313. [Google Scholar] [CrossRef]
38. Hashish, M. Machining of advanced composites with abrasive-waterjets', *ASME Winter Annual Meeting*, Chicago, **1998**. [Google Scholar]
39. Bañon, F.; Sambruno, A.; Batista, M.; Bartolome, S.; Jorge, S. Study of the surface quality of carbon fiber–reinforced thermoplastic matrix composite (CFRTP) machined by abrasive water jet (AWJM). *Int. J. Adv. Manuf. Technol*. **2020**, 107, 3299–3313. [Google Scholar] [CrossRef]
40. Sutowska, M.; Łukianowicz, C.; Szada-Borzyszkowska, M. Sequential Smoothing Treatment of Glass Workpieces Cut by Abrasive Water Jet. *Materials*, **2022**, 15, [Google Scholar] [CrossRef]
41. Sutowska, M.; Kapłonek, W.; Pimenov, D.Y.; Gupta, M.K.; Mia, M.; Sharma, S. Influence of Variable Radius of Cutting Head Trajectory on Quality of Cutting Kerf in the Abrasive Water Jet Process for Soda–Lime Glass. *Materials*, **2020**, 13, 4277. [Google Scholar] [CrossRef]
42. Hashish, M.; Whalen, J. Precision Drilling of Ceramic-Coated Components With Abrasive-Waterjets. ASME. *J. Eng. Gas Turbines Power*. **1993**, 115(1), 148–154. [Google Scholar] [CrossRef]
43. Aydin, G.; Kaya, S.; Karakurt, I. Utilization of solid-cutting waste of granite as an alternative abrasive in abrasive waterjet cutting of marble. *Journal of Cleaner Production*, **2017**, Vol. 159, 241-247. [Google Scholar] [CrossRef]
44. Karakurt, I.; Aydin, G.; Aydiner, K. An experimental study on the depth of cut of granite in abrasive waterjet cutting. *Materials and Manufacturing Processes*, **2012**, 27(5), 538-544. [Google Scholar] [CrossRef]
45. Barabas, S.; Florescu, A. Reduction of Cracks in Marble Appeared at Hydro-Abrasive Jet Cutting Using Taguchi Method. *Materials*, **2022**, 15(2), 486. [Google Scholar] [CrossRef]
46. Huang, C. Z.; Hou, R. G.; Wang, J.; Feng, Y. X. The effect of high pressure abrasive water jet cutting parameters on cutting performance of granite. *In Key Engineering Materials*, Trans Tech Publications Ltd., **2006**, Vol. 304, 560-564). [Google Scholar] [CrossRef]
47. Aydin, G. Recycling of abrasives in abrasive water jet cutting with different types of granite. *Arabian Journal of Geosciences*, **2014**, 7(10), 4425-4435. [Google Scholar] [CrossRef]
48. Perec, A. Research into the disintegration of abrasive materials in the abrasive water jet machining process. *Materials*, **2021**, 14(14), 3940. [Google Scholar] [CrossRef]
49. Perec, A.; Radomska-Zalas, A.; Fajdek-Bieda, A. Experimental Research into Marble Cutting by Abrasive Water Jet. Facta Universitatis, Series: Mechanical Engineering 2022, 20, 145–156, [Google Scholar] [CrossRef]
50. Perec, A. Investigation of Limestone Cutting Efficiency by the Abrasive Water Suspension Jet. In Advances in Manufacturing Engineering and Materials; Hloch, S., Klichová, D., Krolczyk, G.M., Chattopadhyaya, S., Ruppenthalová, L., Eds.; Springer International Publishing: Cham, 2019; pp. 124–134, [Google Scholar] [CrossRef]
51. Radomska-Zalas, A.; Perec, A.; Fajdek-Bieda, A. IT Support for Optimisation of Abrasive Water Cutting Process Using the TOPSIS Method. IOP Conference Series: Materials Science and Engineering 2019, 710, 012008, [Google Scholar] [CrossRef]
52. Perec, A. Multiple Response Optimization of Abrasive Water Jet Cutting Process Using Response Surface Methodology (RSM). Procedia Computer Science 2021, 192, 931–940, [Google Scholar] [CrossRef]

 doi:10.20944/preprints202212.0174.v1

53. Hashish, M. On the modeling of abrasive - waterjet cutting. 7th International Symposium on Jet Cutting Technology. Ottawa, **1984**, 249-265. [Google Scholar]
54. Iioshi, S.; Nakao, K.; Torii, K.; Ishii, T. Preliminary study on abrasive water jet assist roadheader. 8th International Symposium on Jet Cutting Technology. Durham, UK, **1986**, 71-77. [Google Scholar]
55. Rehbinder, G. A theory about cutting rock with a water jet. *Rock mechanics*, **1980**, 12(3), 247-257. [Google Scholar] [CrossRef]
56. Galecki, G.; Summers, D.A.; Sprung, J.; Yount, J. Development of a Waste Excavation End Effector, 12th International Conference on Jet Cutting Technology, Rouen, France, **1994**, 637-647.
57. Xu, J.; Summers, D. A. Experimental evaluation of the performance of fan jet systems. In Proceedings of 12th International Symposium of Jet Cutting Technology, **1994**, (pp. 37-43). [Google Scholar]
58. Racinkowski, R. collective work: Engineering geology with elements of petrography and hydrology. Wydawnictwa Uczelniane Politechniki Szczecińskiej, Szczecin, **1987**.
59. Vijay, M.M.; Wenzhuo, Yan. Water jet cutting techniques for processing of hard rock material, *International Journal of Surface Mining, Reclamation and Environment*, **1989**, 3:2, 59-69, [Google Scholar] [CrossRef]
60. Kukiełka, L. Fundamentals of engineering studies (in Polish), **2002**, Sci. Ed. by PWN, Warsaw, ISBN 8301137495, 9788301137496, 273 pages. [CrossRef]